PHYSICAL REVIEW E **84**, 065301(R) (2011)

Paradoxical transitions to instabilities in hydromagnetic Couette-Taylor flows

Oleg N. Kirillov,[1] Dmitry E. Pelinovsky,[2] and Guido Schneider[3]
[1]*Helmholtz-Zentrum Dresden-Rossendorf, P.O. Box 510119, D-01314 Dresden, Germany*
[2]*Department of Mathematics, McMaster University, Hamilton, Ontario, Canada L8S 4K1*
[3]*Institute of Analysis, Dynamics, and Modeling, University of Stuttgart, Stuttgart, Germany*

(Received 22 August 2011; published 14 December 2011)

By methods of modern spectral analysis, we rigorously find distributions of eigenvalues of linearized operators associated with an ideal hydromagnetic Couette-Taylor flow. The transition to instability in the limit of a vanishing magnetic field has a discontinuous change compared to the Rayleigh stability criterion for hydrodynamical flows, which is known as the Velikhov-Chandrasekhar paradox.

DOI: 10.1103/PhysRevE.84.065301 PACS number(s): 47.35.Tv, 46.15.Ff, 47.32.−y, 47.85.L−

Instabilities of Couette-Taylor (CT) flow between two rotating cylinders are the cornerstone of 20th century studies of hydrodynamics [1]. In 1917 Rayleigh found a necessary and sufficient condition for the centrifugal instability of CT flow of an ideal fluid between cylinders of infinite length with respect to axisymmetric perturbations [2]. Taylor extended Rayleigh's result to viscous CT flow and computed seminal linear stability diagrams that perfectly agreed with the experiment at moderate angular velocities [3].

Despite the fact that the Couette-Taylor flow has been studied, theoretically and experimentally, for more than a century, the past decade has seen a true renaissance of this classical subject caused by increased demands for active development of laboratory experiments with liquid metals that rotate in an external magnetic field [4]. The prevalence of resistive dissipation over viscous dissipation in liquid metals dictates unprecedentedly high values of the Reynolds number ($\mathrm{Re} \sim 10^6$) at the threshold of the *magnetorotational instability* (MRI) of hydrodynamically stable quasi-Keplerian flows, which is currently considered to be the most probable trigger of turbulence in astrophysical accretion disks [5]. Difficulties in keeping hydrodynamical CT flows laminar at such high speeds puts the laboratory detection of MRI at the edge of modern technical capabilities.

Is the existing theory of MRI well prepared to face these promising experimental opportunities? No matter how paradoxical it may sound, the answer is "not yet."

Indeed, the discoverers of MRI, Velikhov [6] and Chandrasekhar [7], pointed out a counterintuitive phenomenon. In the case of an ideal nonresistive flow, which we consider in this Rapid Communication, boundaries of the region of the magnetorotational instability are misplaced compared to the Rayleigh boundaries of the region of the centrifugal instability, and do not converge to those in the limit of a negligibly small axial magnetic field. Nevertheless, the convergence is possible in the presence of dissipation and resistivity [8].

Existing attempts to physically explain the *Velikhov-Chandrasekhar paradox* [9] involve Alfvén's theorem, which "attaches" magnetic field lines to a fluid of zero electrical resistivity, independent of the strength of the magnetic field, which implies conservation of the angular velocity (Velikhov-Chandrasekhar) rather than the angular momentum (Rayleigh). However, the weak point of this argument is that the actual boundary of MRI does depend on the magnetic field strength even in the case of ideal magnetohydrodynamics (MHD) and tends to that of solid body rotation only when the field is vanishing. This indicates that the roots of the paradox are more hidden.

Recently, this intriguing effect was reconsidered in the full viscous and resistive setting by a local Wentzel-Kramers-Brillouin (WKB) approximation [10]. It was found that the threshold surface of MRI in the space of resistive frequency, Alfvén frequency and Rossby number possesses a structurally stable singularity known as the *Plücker conoid*, which persists at any level of viscous dissipation. The singular surface connects the Rayleigh- and the Velikhov-Chandrasekhar thresholds through the continuum of intermediate states parametrized by the Lundquist number [10].

Why does this singularity exist? Our Rapid Communication sheds light on this question via rigorous inspection of the spectra of the boundary eigenvalue problems associated with the ideal hydrodynamic and hydromagnetic CT flows. Rigorous spectral results are illustrated by MATLAB computations of eigenvalues of the linearized operators.

If $\mathbf{u}$ is the velocity field, $\mathbf{b}$ is the magnetic field, and cylindrical coordinates (r,θ,z) are used, the basic CT flow between cylinders of radii R_1 and R_2, $R_1 < R_2$, is

$$\mathbf{u}_0 = r\Omega(r)\mathbf{e}_\theta, \quad \mathbf{b}_0 = b_0\mathbf{e}_z, \quad \Omega(r) = a + cr^{-2}, \tag{1}$$

where b_0 is arbitrary and (a,c) are related uniquely to $\Omega_{1,2} = \Omega(R_{1,2})$ through the viscous limit

$$a = \frac{\Omega_2 R_2^2 - \Omega_1 R_1^2}{R_2^2 - R_1^2}, \quad c = \frac{(\Omega_1 - \Omega_2)R_1^2 R_2^2}{R_2^2 - R_1^2}. \tag{2}$$

In the case of co-rotating cylinders $\Omega_{1,2} > 0$, the Rayleigh boundary corresponds to $a = 0$, whereas the Velikhov-Chandrasekhar boundary is $c = 0$.

The summary of our results is as follows.

(I) In the case of no magnetic field ($b_0 = 0$), co-rotating cylinders ($\Omega_{1,2} > 0$), and an ideal fluid, we prove that the linearized stability problem has a countable set of neutrally stable pairs of (purely imaginary) eigenvalues for $a > 0$ and a set of unstable pairs of (purely real) eigenvalues for $a < 0$, all accumulating to zero. At $a = 0$, all pairs of eigenvalues merge together at zero.

(II) Under the same conditions but for counter-rotating cylinders with $\Omega_1 < 0$ and $\Omega_2 > 0$, we show that there exist two sets of eigenvalue pairs: One set contains real eigenvalues and the other set contains purely imaginary eigenvalues. The unstable real eigenvalues converge to the zero accumulation point when $\Omega_1 \to 0$ for fixed $\Omega_2 > 0$ (where $a > 0$), whereas the stable imaginary eigenvalues persist across $\Omega_1 = 0$.

(III) For any magnetic field ($b_0 \neq 0$), co-rotating cylinders ($\Omega_{1,2} > 0$), and an ideal nonresistive hydromagnetic flow, we prove that there exist two sets of eigenvalue pairs and both sets contain only purely imaginary eigenvalues for $0 < \Omega_1 < \Omega_2$. One set remains purely imaginary for $\Omega_1 > \Omega_2$ but the other set transforms to the set of real eigenvalues along a countable sequence of curves, which are located for $\Omega_1 > \Omega_2$ and approach the diagonal line $\Omega_1 = \Omega_2$ ($c = 0$) in the limit $b_0 \to 0$. One pair of purely imaginary eigenvalues below the corresponding curve transforms into a pair of unstable real eigenvalues above the curve. No eigenvalues pass through the origin of the complex plane in the neighborhood of the line $a = 0$, even if b_0 is close to zero.

(IV) Under the same conditions but for counter-rotating cylinders with $\Omega_1 < 0$ and $\Omega_2 > 0$, we show the existence of four sets of eigenvalue pairs, which are either purely imaginary or real. The unstable eigenvalues bifurcate again along a countable sequence of curves, which are located for $\Omega_1 < 0$ and approach $\Omega_1 = 0$ in the limit $b_0 \to 0$. The purely imaginary pair of eigenvalues above the curve turns into a purely real pair of eigenvalues below the curve.

Although the results (I) and (II) partially reproduce the conclusions of Synge [11], the existence of zero eigenvalues of infinite multiplicity at the Rayleigh threshold is emphasized here. A similar coalescence of all eigenvalues at the zero value occurs also in the Bose-Hubbard dimer [12]. Results (III) and (IV) are unique, to the best of our knowledge. Numerical evidence of these results can be found in Ref. [13].

The rest of our Rapid Communication is devoted to the proofs of the above results and their numerical illustrations. We take the equations for an ideal hydromagnetic fluid [9]

$$\begin{aligned} \mathbf{u}_t + (\mathbf{u}\cdot\nabla)\mathbf{u} &= -\nabla\left(p + \tfrac{1}{2}|\mathbf{b}|^2\right) + (\mathbf{b}\cdot\nabla)\mathbf{b}, \\ \mathbf{b}_t &= \nabla\times(\mathbf{u}\times\mathbf{b}), \\ \nabla\cdot\mathbf{u} &= 0, \quad \nabla\cdot\mathbf{b} = 0, \end{aligned} \tag{3}$$

where p is the pressure term determined from the incompressibility condition $\nabla\cdot\mathbf{u} = 0$. We linearize (3) at the basic flow (1) and use the standard separation of variables for symmetric (θ-independent) perturbations

$$\mathbf{u} = \mathbf{u}_0 + \mathbf{U}(r)e^{\gamma t + ikz}, \quad \mathbf{b} = \mathbf{b}_0 + \mathbf{B}(r)e^{\gamma t + ikz}, \tag{4}$$

where γ is the growth rate of perturbations in time and $k \in \mathbb{R}$ is the Fourier wave number with respect to the cylindrical coordinate z. Performing routine calculations [8], we find the system of four coupled equations for components of $\mathbf{U}$ and $\mathbf{B}$ in the directions of $\mathbf{e}_r$ and $\mathbf{e}_\theta$ (denoted by U_r, U_θ, B_r, and B_θ)

$$\begin{aligned} ikb_0(k^2+L)B_r + 2k^2\Omega(r)U_\theta &= \gamma(k^2+L)U_r, \\ ikb_0B_\theta - 2aU_r &= \gamma U_\theta, \\ ikb_0U_r &= \gamma B_r, \\ ikb_0U_\theta - \frac{2c}{r^2}B_r &= \gamma B_\theta, \end{aligned} \tag{5}$$

where $L = -\partial_r^2 - \frac{1}{r}\partial_r + \frac{1}{r^2}$ is the Bessel operator, which is strictly positive and self-adjoint with respect to the weighted inner product $\langle f,g\rangle = \int_{R_1}^{R_2} rf(r)g(r)dr$. We note that the z components of $\mathbf{U}$ and $\mathbf{B}$, as well as the pressure term, have been eliminated from the system of equations (5) under the condition $k \neq 0$.

For hydrodynamic instabilities of the CT flow, we set $b_0 = 0$, which yields uniquely $B_r = B_\theta = 0$, $2aU_r + \gamma U_\theta = 0$, and a closed linear eigenvalue problem

$$\gamma^2(k^2+L)U_r = -4k^2a\Omega(r)U_r, \quad R_1 < r < R_2, \tag{6}$$

subject to the Dirichlet boundary conditions at the inner and outer cylinders $U_r(R_1) = U_r(R_2) = 0$.

The operator L is an unbounded strictly positive operator with a purely discrete spectrum of positive eigenvalues $\{\mu_n\}_{n\in\mathbb{N}}$ that diverge to infinity according to the distribution $\mu_n = \mathrm{O}(n^2)$ as $n \to \infty$. Inverting this operator for any real k and defining a different eigenfunction Ψ by $U_r = (k^2 + L)^{-1/2}\Psi$, we rewrite (6) in the form

$$\gamma^2\Psi = -aT\Psi, \quad T = 4k^2(k^2+L)^{-1/2}\Omega(k^2+L)^{-1/2}, \tag{7}$$

where the self-adjoint compact operator T has eigenvalues $\{-\gamma^2/a\}_{n\in\mathbb{N}}$ that accumulate to zero with $\gamma_n = O(n^{-1})$ as $n \to \infty$.

If $\Omega_1,\Omega_2 > 0$, then $\Omega(r) > 0$ for all $r \in [R_1,R_2]$ and T is a compact positive operator. Hence, all $\gamma_n^2 < 0$ if $a > 0$ and all $\gamma_n^2 > 0$ if $a < 0$. The condition $a = 0$ ($\Omega_2R_2^2 = \Omega_1R_1^2$) is the Rayleigh boundary, at which all eigenvalues are at $\gamma = 0$. The proof of (I) is complete.

If $\Omega_1 < 0$ and $\Omega_2 > 0$, then $a > 0$ but Ω is sign indefinite on $[R_1,R_2]$. Since T is a compact sign-indefinite operator, it has two sequences of eigenvalues accumulating to zero: One sequence has $\gamma_n^2 < 0$ and the other one has $\gamma_n^2 > 0$. This completes the proof of (II).

Figure 1(a) gives numerical approximations of the five positive and five negative squared eigenvalues γ^2 as functions of the parameter Ω_1 for fixed values of $\Omega_2 = 1$, $R_1 = 1$, $R_2 = 2$, and $k = 1$. The dotted line shows the accumulation point $\gamma = 0$ for the sequences of eigenvalues.

For hydromagnetic instabilities, we express B_r, B_θ, and U_θ from the system of linearized equations (5) and find a closed linear eigenvalue problem

$$\left(\gamma^2 + k^2b_0^2\right)^2(k^2+L)U_r = 4k^2\Omega(r)\left(\frac{k^2b_0^2c}{r^2} - a\gamma^2\right)U_r, \tag{8}$$

subject to the same Dirichlet boundary conditions at $r = R_{1,2}$. If $b_0 = 0$ and $\gamma \neq 0$, system (8) reduces to (6), however, it is a biquadratic eigenvalue problem and hence has a double set of eigenvalues compared to (6).

Denoting $\lambda = \gamma^2 + k^2b_0^2$, we rewrite (8) as the quadratic eigenvalue problem

$$\lambda^2(k^2+L)U_r + 4ak^2\lambda\Omega(r)U_r = 4k^4b_0^2\Omega^2(r)U_r. \tag{9}$$

It follows again from the compactness of the operators $(k^2+L)^{-1}\Omega$ and $(k^2+L)^{-1}\Omega^2$ that the spectrum of

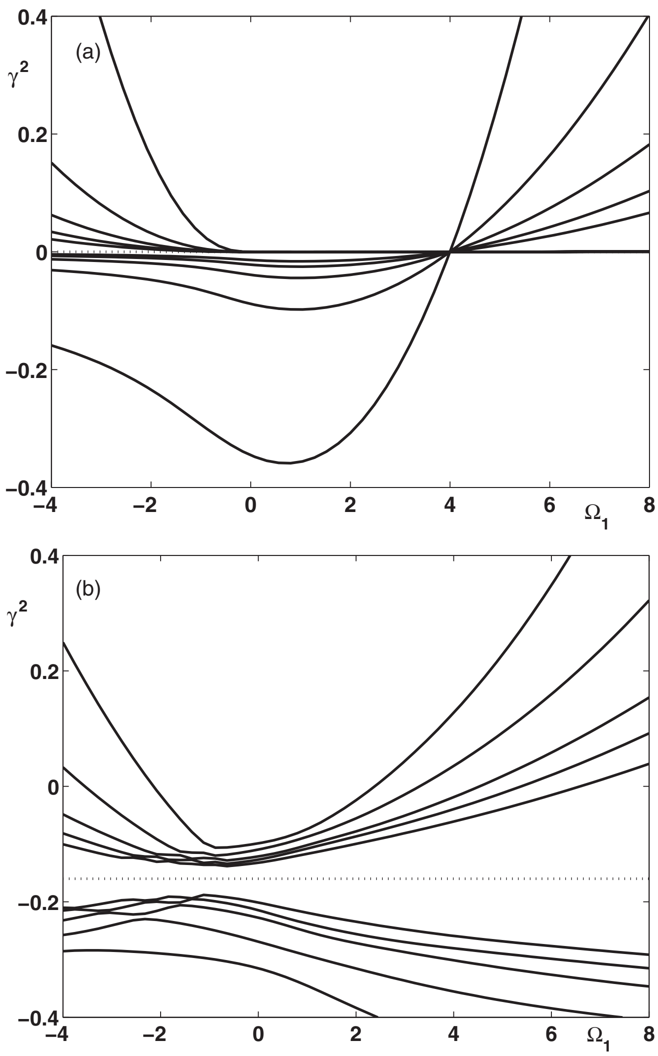

FIG. 1. Squared eigenvalues γ^2 of problem (8) vs Ω_1 for $\Omega_2 = 1$, $R_1 = 1$, $R_2 = 2$, and $k = 1$. (a) $b_0 = 0$: All squared eigenvalues γ coalesce to zero at the Rayleigh line $\Omega_1 R_1^2 = \Omega_2 R_2^2$, whereas positive squared eigenvalues for $\Omega_1 < 0$ merge to zero at $\Omega_1 = 0$. (b) $b_0 = 0.4$: The squared eigenvalues change stability above the Velikhov-Chandrasekhar line $\Omega_1 = \Omega_2$ and below $\Omega_1 = 0$.

the quadratic eigenvalue problem (9) is purely discrete. Chandrasekhar [7] showed that all eigenvalues λ are real. We shall prove that these eigenvalues accumulate to zero as two countable sets with $\lambda_n = O(n^{-1})$ as $n \to \infty$, one set is for positive λ and the other set is for negative λ. The result definitely holds for $a = 0$ because λ^2 becomes an eigenvalue of the self-adjoint problem

$$\lambda^2 \Psi = k^2 b_0^2 S \Psi, \quad S = 4k^2 (k^2 + L)^{-1/2} \Omega^2 (k^2 + L)^{-1/2}, \tag{10}$$

where S is a self-adjoint compact positive operator.

To show the same conclusion for $a \neq 0$, we use a recently developed technique from Ref. [14] and rewrite (9) as a parameter continuation problem for $\nu = \lambda^{-1}$,

$$a\nu \Omega(r) U_r = -\frac{1}{4k^2}(k^2 + L) U_r + k^2 b_0^2 \epsilon^2 \Omega^2(r) U_r. \tag{11}$$

Here eigenvalues ν of (11) for $a \neq 0$ are continued with respect to the real values of ϵ to recover eigenvalues $\lambda = \nu^{-1}$ of (9) at the intersections with the diagonal $\nu = \epsilon$.

At $\epsilon = 0$, we recover the hydrodynamical problem (6). If $\Omega_1, \Omega_2 > 0$, then $\Omega(r) > 0$ for all $r \in [R_1, R_2]$ and eigenvalues $\{\nu_n(\epsilon)\}_{n\in\mathbb{N}}$ at $\epsilon = 0$ are strictly negative if $a > 0$ or strictly positive if $a < 0$. Moreover, $\nu_n(0) = O(n^2)$ as $n \to \infty$. Without loss of generality, let us consider the case $a > 0$. Each negative eigenvalue $\nu_n(\epsilon)$ is strictly increasing for large values of $|\epsilon|$ at any point ϵ_0, because

$$a\epsilon_0 \left.\frac{d\nu_n}{d\epsilon}\right|_{\epsilon=\epsilon_0} = 2\epsilon_0^2 k^2 b_0^2 \frac{\langle \Omega^2 \varphi_n, \varphi_n \rangle}{\langle \Omega \varphi_n, \varphi_n \rangle} > 0, \tag{12}$$

where φ_n is the eigenfunction for the eigenvalue $\nu_n(\epsilon)$ in Eq. (11) at $\epsilon = \epsilon_0$. The right-hand side of (12) is always bounded, hence the eigenvalues $\{\nu_n(\epsilon)\}_{n\in\mathbb{N}}$ are continued to positive infinity as $|\epsilon| \to \infty$. As a result, there exist two countable sets of intersections of eigenvalues $\{\nu_n(\epsilon)\}_{n\in\mathbb{N}}$ with $\nu = \epsilon$: One set is for positive $\lambda = \nu^{-1}$ and the other set is for negative λ. Both sets accumulate at zero as $n \to \infty$. This completes the proof of (III).

If $\Omega_1 < 0$ and $\Omega_2 > 0$, then $a > 0$ but Ω is sign indefinite on $[R_1, R_2]$. In this case, again using the compact operator T in Eq. (7), there exist two sets of eigenvalues $\{\nu_n^{\pm}(\epsilon)\}_{n\in\mathbb{N}}$ of (11) at $\epsilon = 0$: One set $\{\nu_n^{-}(0)\}_{n\in\mathbb{N}}$ is strictly negative with $\langle \Omega\varphi_n^-, \varphi_n^- \rangle > 0$ and the other set $\{\nu_n^{+}(0)\}_{n\in\mathbb{N}}$ is strictly positive with $\langle \Omega\varphi_n^+, \varphi_n^+ \rangle < 0$. Because the signs of $\langle \Omega\varphi_n^\pm, \varphi_n^\pm \rangle$ are preserved for small $\epsilon \neq 0$, it follows from the derivative (12) that the eigenvalues $\{\nu_n^{-}(\epsilon)\}_{n\in\mathbb{N}}$ are convex upward for larger values of $|\epsilon|$ and the eigenvalues $\{\nu_n^{+}(\epsilon)\}_{n\in\mathbb{N}}$ are concave downward for larger values of ϵ. The curves of $\{\nu_n^{\pm}(\epsilon)\}_{n\in\mathbb{N}}$ may intersect but the intersection is safe (i.e., eigenvalues split without the onset of complex eigenvalues) because the eigenvalue problem (11) is self-adjoint for any real ϵ and hence multiple eigenvalues are always semisimple. If the signs of $\langle \Omega\varphi_n^\pm, \varphi_n^\pm \rangle$ are preserved along the entire curves, then we conclude on the existence of four sets of intersections of these eigenvalues with the main diagonal $\nu = \epsilon$: Two sets give positive eigenvalues λ and the two other sets give negative eigenvalues. The conclusion is not affected by the fact that $\langle \Omega\varphi_n^\pm, \varphi_n^\pm \rangle$ may vanish along the curve. If this has occurred, then $\langle \Omega\varphi_n^\pm, \varphi_n^\pm \rangle$ has at least a simple zero due to analyticity in ϵ and hence the derivative (12) is infinite, which implies that the corresponding curve $\nu_n^{\pm}(\epsilon)$ goes to plus or minus infinity for finite values of ϵ. This argument completes the proof of (IV).

Figure 1(b) shows numerical approximations of the five positive and five negative squared eigenvalues γ^2 as functions of Ω_1 for fixed values of $\Omega_2 = 1$, $R_1 = 1$, $R_2 = 2$, $b_0 = 0.4$, and $k = 1$. Cascades of instabilities arise for $\Omega_1 > \Omega_2$ and $\Omega_1 < 0$ by subsequent merging of pairs of purely imaginary eigenvalues γ at the origin and splitting into pairs of real (unstable) eigenvalues γ. For $\Omega_1 > 0$, the two sets of squared eigenvalues accumulate to the value $\gamma^2 = -k^2 b_0^2$ $(\lambda = 0)$, which is shown by the dotted line. For $\Omega_1 < 0$, a more complicated behavior is observed within each set: The squared eigenvalues coalesce and split safely, indicating that each set is actually represented by two disjoint sets of the squared eigenvalues.

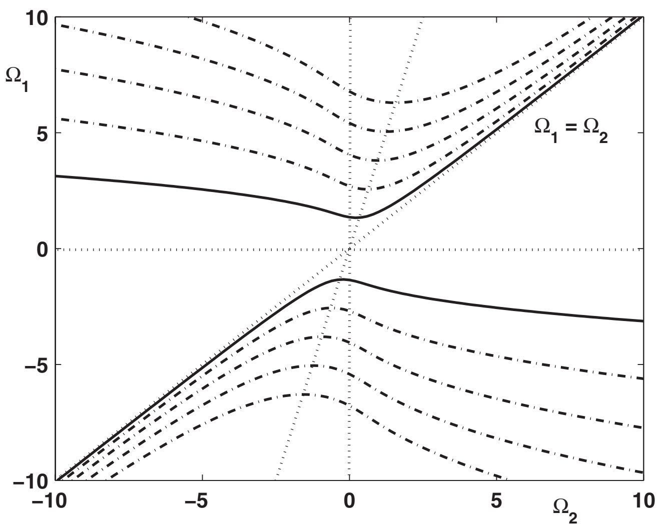

FIG. 2. Curves of zero eigenvalues (the stability domain is located between solid curves) for $R_1 = 1$, $R_2 = 2$, $b_0 = 0.4$, and $k = 1$. The curves approach the line $\Omega_1 = \Omega_2$ as $b_0 \to 0$.

To study the instability boundaries in Eq. (8), we substitute $\gamma = 0$ and regroup terms for $b_0 \neq 0$ to obtain

$$b_0^2(k^2 + L)U_r = 4(\Omega_1 - \Omega_2)\frac{R_1^2 R_2^2 \Omega(r)}{(R_2^2 - R_1^2)r^2}U_r. \qquad (13)$$

If $\Omega_{1,2} > 0$, it follows from Eq. (13) that there exists a countable set of bifurcation curves for $\Omega_1 > \Omega_2$, because L is a positive operator and $\Omega(r)$ is strictly positive. On the other hand, in the quadrant $\Omega_1 < 0$ and $\Omega_2 > 0$, there exists another set of bifurcation curves, because Ω is sign indefinite and L is unbounded.

To study further the instability boundaries, we notice that $\Omega(r)$ depends on both Ω_1 and Ω_2. Therefore, we shall rewrite (13) as the quadratic eigenvalue problem with the unique eigenvalue parameter c in Eq. (2)

$$b_0^2(k^2 + L)U_r = \frac{4\Omega_2}{r^2}cU_r + \frac{4}{r^2}\left(\frac{1}{r^2} - \frac{1}{R_2^2}\right)c^2U_r. \qquad (14)$$

Figure 2 shows numerical approximations of the first five curves of zero eigenvalues in the upper half of the (Ω_1,Ω_2) plane for fixed values of $R_1 = 1$, $R_2 = 2$, $b_0 = 0.4$, and $k = 1$ and their mirror reflections in the lower half plane. The dotted curves show the diagonal line $\Omega_1 = \Omega_2$, the Rayleigh line $\Omega_1 R_1^2 = \Omega_2 R_2^2$, as well as the axes $\Omega_1 = 0$ and $\Omega_2 = 0$. It is clear that each curve approaches the diagonal line $\Omega_1 = \Omega_2$ for large values of $\Omega_{1,2}$. When b_0 becomes small, they approach closely to the line $\Omega_1 = \Omega_2$.

The above conclusions also follow from a rigorous analysis of the quadratic eigenvalue problem (14). In the limit $\Omega_2 \to \infty$, we can set $\lambda = \Omega_2 c$ as a unique eigenvalue and treat the last term in Eq. (14) as a small bounded perturbation to the unbounded operator. In the limit $b_0 \to 0$, we set $c = b_0^2\lambda$ and again treat the last term in Eq. (14) as a small perturbation. In both cases, eigenvalues λ approach to the first eigenvalues of the positive unbounded operator $r^2(k^2 + L)$. We note that this approximation is not uniform for all bifurcation curves and only applies to the finitely many bifurcation curves.

To summarize, we gave mathematically rigorous proofs of the distributions and bifurcations of eigenvalues of linearized operators associated with an ideal hydromagnetic CT flow. This work lays a firm basis for perturbation theory in small dissipation and resistivity that will enable an identification of unstable modes of the nonideal MRI.

O.K. thanks Frank Stefani for fruitful discussions. D.P. is supported by the AvH Foundation. G.S. is supported by DFG through the Excellence cluster SimTech.

[1] P. Chossat and G. Iooss, *The Couette-Taylor Problem* (Springer, New York, 1994); R. Tagg, Nonlin. Sci. Today **4**, 1 (1994).
[2] J. W. S. Rayleigh, Proc. R. Soc. London A **93**, 148 (1917).
[3] G. I. Taylor, Philos. Trans. R. Soc. London A **223**, 289 (1923).
[4] H. Ji, M. Burin, E. Schartman, and J. Goodman, Nature (London) **444**, 343 (2006); F. Stefani *et al.*, Phys. Rev. Lett. **97**, 184502 (2006); F. Stefani, A. Gailitis, and G. Gerbeth, ZAMM **88**, 930 (2008); M. D. Nornberg, H. Ji, E. Schartman, A. Roach, and J. Goodman, Phys. Rev. Lett. **104**, 074501 (2010); H. Ji, Proc. Int. Astron. Union **6**, 18 (2010); M. S. Paoletti and D. P. Lathrop, Phys. Rev. Lett. **106**, 024501 (2011); S. Balbus, Nature (London) **470**, 475 (2011).
[5] S. A. Balbus and J. F. Hawley, Astrophys. J. **376**, 214 (1991); Rev. Mod. Phys. **70**, 1 (1998).
[6] E. P. Velikhov, Sov. Phys. JETP **9**, 995 (1959).
[7] S. Chandrasekhar, Proc. Natl. Acad. Sci. USA **46**, 253 (1960).
[8] Th. Gebhardt and S. Grossmann, Z. Phys. B **90**, 475 (1993); G. Rüdiger and Y. Zhang, Astron. Astrophys. **378**, 302 (2001); H. Ji, J. Goodman, and A. Kageyama, Mon. Not. R. Astron. Soc. **325**, L1 (2001); A. P. Willis and C. F. Barenghi, Astron. Astrophys. **388**, 688 (2002); I. Herron, Anal. Appl. **2**, 145 (2004); B. Dubrulle *et al.*, Phys. Fluids **17**, 095103 (2005).
[9] D. J. Acheson and R. Hide, Rep. Progr. Phys. **36**, 159 (1973); E. Knobloch, Mon. Not. R. Astron. Soc. **255**, 25 (1992); S. A. Balbus, Annu. Rev. Astron. Astrophys. **41**, 555 (2003); E. P. Velikhov, JETP Lett. **82**, 690 (2005); D. A. Shalybkov, Phys. Usp. **52**, 915 (2009).
[10] O. N. Kirillov and F. Stefani, Astrophys. J. **712**, 52 (2010); Phys. Rev. E **84**, 036304 (2011).
[11] J. L. Synge, Trans. R. Soc. Can., Sect. 3 **27**, 1 (1933); P. G. Drazin and W. H. Reid, *Hydrodynamic Stability* (Cambridge University Press, Cambridge, UK, 1981).
[12] E. M. Graefe *et al.*, J. Phys. A **41**, 255206 (2008); A. A. Sukhorukov, Z. Xu, and Yu. S. Kivshar, Phys. Rev. A **82**, 043818 (2010); K. Li and P. G. Kevrekidis, Phys. Rev. E **83**, 066608 (2011).
[13] R. Keppens, F. Casse, and J. P. Goedbloed, Astrophys. J. **569**, L121 (2002).
[14] R. Kollar, SIAM J. Math. Anal. **43**, 612 (2011).